Sinensetin suppresses angiogenesis in liver cancer by targeting the VEGF/VEGFR2/AKT signaling pathway

XIAO LI[1], YAN LI[1], YUAN WANG[1], FUHONG LIU[2], YANJUN LIU[1], JIANGJIU LIANG[3], RUCAI ZHAN[4], YUE WU[1], HE REN[1], XIUYUAN ZHANG[1] and JU LIU[1,2]

[1]College of Traditional Chinese Medicine, Shandong University of Traditional Chinese Medicine, Jinan, Shangdong 250355; [2]Laboratory of Microvascular Medicine, Medical Research Center, The First Affiliated Hospital of Shandong First Medical University and Shandong Provincial Qianfoshan Hospital; [3]Department of Gerontology, The First Affiliated Hospital of Shandong First Medical University; [4]Department of Neurosurgery, The First Affiliated Hospital of Shandong First Medical University, Jinan, Shandong 250014, P.R. China

Received January 16, 2022; Accepted March 15, 2022

DOI: 10.3892/etm.2022.11287

Abstract. Sinensetin (SIN) is a polymethoxy flavone primarily present in citrus fruits. This compound has demonstrated anticancer activity. However, the underlying mechanism of its action has not been fully understood. The present study investigated the impact of SIN on angiogenesis in a liver cancer model. In a murine xenograft tumor model, SIN inhibited the growth of HepG2/C3A human liver hepatoma cell-derived tumors and reduced the expression levels of platelet/endothelial cell adhesion molecule-1 and VEGF. In HepG2/C3A cells, SIN repressed VEGF expression by downregulating hypoxia-inducible factor expression. In cultured human umbilical vein endothelial cells, SIN increased apoptosis and repressed migration and tube formation. In addition, SIN decreased the phosphorylation of VEGFR2 and inhibited the AKT signaling pathway. Molecular docking demonstrated that the VEGFR2 core domain effectively combined with SIN at various important residues. Collectively, these data suggested that SIN inhibited liver cancer angiogenesis by regulating VEGF/VEGFR2/AKT signaling.

Introduction

Angiogenesis is required for tumor development (1). This process involves the interaction between various cell types and molecules, contributing to basement membrane degradation, endothelial cell (EC) migration and proliferation and tube formation (2). As one of the primary malignant tumors with high mortality rates worldwide, liver cancer is characterized by an abundant blood supply (3). Therefore, liver cancer angiogenesis is a therapeutic target (4,5). New agents of anti-angiogenic therapy are greatly required.

Sinensetin (SIN) is a polymethoxy flavone containing five methoxy groups that is present mainly in citrus fruits (6). Previous studies have demonstrated that SIN can inhibit the development of several malignant tumors, such as gallbladder adenocarcinoma, T-cell lymphoma and gastric cancer (7-9). A recent study revealed that SIN may be a potential anticancer drug targeting autophagy of hepatocellular carcinoma (10). However, the effects of SIN on liver cancer angiogenesis remain to be elucidated.

Angiogenesis is regulated by various angiogenic factors, such as VEGF and its receptor (11), platelet-derived growth factor and angiopoietin (12-14). Among them, VEGFRs are the key mediators of angiogenesis (15). VEGF is mainly produced by tumor cells, notably found in benign and malignant lesions (16). The increase in VEGF expression induced by tumor secretion is caused by specific hypoxia-inducible factors (HIFs) (17). As a receptor of VEGF, VEGFR is mainly located on the EC membrane and has the three following types: VEGFR1, VEGFR2 and VEGFR3. VEGFR2 is mainly present in vascular ECs (18). VEGF is released by tumor cells and can bind to VEGFR2 on ECs, causing its autophosphorylation. Following phosphorylation at Tyr1175 of VEGFR2, the latter binds to the p85 subunit of phosphoinositide-3-kinase (PI3K) and activates the PI3K-AKT signaling pathway (19). However, it remains unclear whether SIN can block the signal transduction of VEGF/VEGFR2 and eventually lead to inhibition of angiogenesis in liver cancer.

The present study observed that SIN inhibited the growth and angiogenesis of HepG2/C3A-derived tumors *in vivo*. *In vitro* experiments revealed that SIN reduced VEGF through HIF1-α in the hepatoblastoma cell line HepG2/C3A. In addition, it was observed that SIN promoted apoptosis and inhibited proliferation in human umbilical vein endothelial

Correspondence to: Professor Ju Liu, Laboratory of Microvascular Medicine, Medical Research Center, The First Affiliated Hospital of Shandong First Medical University and Shandong Provincial Qianfoshan Hospital, 16766 Jingshi Road, Jinan, Shandong 250014, P.R. China
E-mail: ju.liu@sdu.edu.cn

Key words: sinensetin, angiogenesis, liver cancer, human umbilical vascular endothelial cell, molecular mechanism

cells (HUVECs), causing the repression of invasiveness and pro-angiogenic process of ECs. Moreover, SIN downregulated VEGFR2 phosphorylation and the expression levels of its downstream targets in ECs. The data indicated that SIN may inhibit angiogenesis by regulating the VEGF/VEGFR2/AKT signaling pathway.

Materials and methods

Chemicals and reagents. The antibody against VEGF was purchased from Novus Biologicals. The primary antibodies including anti-VEGFR2 (cat. no. 9698), anti-phosphorylated (p)-VEGFR2 (Tyr1175) (cat. no. 3770), anti-AKT (cat. no. 4691), anti-p-AKT (Ser473) (cat. no. 4060), anti-platelet/endothelial cell adhesion molecule-1 (CD31) (cat. no. 77699), β-actin (cat. no. 4970), GAPDH (cat. no. 2118) and α-tubulin (cat. no. 2125) were acquired from Cell Signaling Technology, Inc.; anti-HIF-1α (cat. no. 20960-1-AP) was provided by ProteinTech Group, Inc. Synthetic SIN (>98% purity; cat. no. SS8550) was purchased from Beijing Solarbio Science & Technology Co. Ltd. and characterized by mass spectrometry. Recombinant human VEGF (VEGF165; cat. no. 100-20) and insulin-like growth factor 1 (IGF-1; cat. no. 100-11) were purchased from PeproTech, Inc. SU1498 (cat. no. HY-19326) is a selective VEGFR2 inhibitor, which was obtained from MedChemExpress.

Xenograft tumor growth assay. A total of 10 male BALB/c nude mice (age, 4 weeks; weight, 15-20 g) purchased from Beijing Weitong Lihua Biotechnology Co., Ltd., were used for the tumor xenograft growth assay. Mice were housed at room temperature (22±1˚C) with 50% humidity under special pathogen-free conditions with a 12-h light/dark schedule. All animal studies were conducted with approval (no. 2017-106) obtained from the Ethics Committee of Shandong Provincial Qianfoshan Hospital. HepG2/C3A cells (ATCC) ($5x10^7$/ml) suspended in 0.2 ml 1:1 serum-free DMEM and Matrigel (Corning, Inc.) were implanted into the right flank of the mice (20). When the tumor size reached a volume of 100 mm^3 (approximately two weeks), tumor-bearing mice were randomized into two groups (n=5, each group). The experimentalgroupmice were administered with SIN (40 mg/kg) (21) by gavage every day for 14 days and the control group received the same volume of 0.9% normal saline for 14 days. Animal health and behavior were monitored daily. The tumor diameter was measured by a slide caliper and the body weight was recorded every two days. The maximum diameter of the observed tumors was 17 mm. The tumor size was calculated with the following formula: Length x $width^2$ x 0.5. Tumors exceeding 10% of the body weight of mice or became infected were used as humane endpoints. Animals were euthanized using 30% volume/min CO_2 upon reaching experimental or humane endpoints. None of nude mice died during the experiment. Following 14 days, the tumors were harvested and subsequently used for western blot and immunohistochemical (IHC) analyses. The duration of the experiment was 4 weeks from the start of the experiment. Cell inoculation and sample collection were performed under anesthesia using 1% (w/v) pentobarbital sodium (40 mg/kg) injections intraperitoneally and all efforts were made to minimize suffering, discomfort and distress.

IHC assay. The tumors were fixed overnight in 4% formaldehyde at room temperature, and then ethanol was used for dehydration at the conventional gradient, xylene for vitrification and paraffin for embedding. Sections (5 μm) were created and deparaffinized with graded xylene and rehydrated by graded ethanol. Following heat-induced antigen retrieval in citrate buffer (pH 6.0) in a high-pressure sterilizer at 121˚C for 10 min, the slides were treated with 3% hydrogen peroxide to quench endogenous peroxidase activity and subsequently incubated with 4% bovine serum albumin at 37˚C for 30 min. The tumor tissue slides were incubated with primary anti-CD31 antibodies (1:100) at 4˚C overnight and washed with PBS three times. HRP-labeled secondary antibody from the MaxVision™ HRP-Polymer anti-mouse/rabbit IHC kit (ready to use; cat. no. KIT5020; Fuzhou Maixin Biotech Co., Ltd.) was applied and incubated for 30 min at room temperature. The slides were then dehydrated in an ascending graded series of absolute ethyl alcohols, cleared in xylene and cover-slipped with neutral balsam. Following treatment with hematoxylin for 2 min at room temperature to stain the nuclei, images were captured using a light microscope and in ten random fields at x200 magnification.

Cell culture. HUVECs (cat. no. PCS-100-010) and HepG2/C3A (cat. no. CRL-10741) cells were purchased from the American Type Culture Collection. HUVECs were incubated in Endothelial Cell Medium (ECM; ScienCell Research Laboratories, Inc.) containing 5% fetal bovine serum (FBS; Gibco; Thermo Fisher Scientific, Inc.) and 1% EC growth supplement (ECGS; ScienCell Research Laboratories, Inc.) at 37˚C. HepG2/C3A cells were incubated in Dulbecco's modified Eagle's medium (HyClone; Cytiva) comprising 10% FBS in a hypoxic incubator with 94% N_2, 5% CO_2 and 1% O_2 at 37˚C.

Proliferation assay. HUVECs were harvested and seeded into 96-well plates at a density of $5x10^3$ cells/well and exposed to various concentrations of SIN (3, 10, 30, 60 and 100 μM). Following culture for 24 h, the viability of HUVECs was detected using CCK-8 (Dojindo Molecular Technologies, Inc.). The optical density, which represented the proliferation of HUVECs, was measured at 450 nm using a Spectra Max 190 (Molecular Devices, LLC).

Apoptosis assay. The induction of apoptosis in HUVECs was assessed using Annexin V-FITC and propidium iodide staining (ELabscience Biotechnology, Inc.). Following treatment with SIN, HUVECs were collected and resuspended in a binding buffer at a final concentration of $1x10^6$ cells/ml. Single cells were incubated with 5 μl Annexin V-FITC and 5 μl PI for 15 min at room temperature in the dark. The percentages of early and late apoptotic cells were assessed using a FACSAria II flow cytometer (BD Biosciences) to calculate the apoptotic rate. Data were analyzed using FlowJo (V10; FlowJo LLC).

Wound healing assay. Migration was assessed using a scratch wound healing assay. The cells were seeded ($4x10^5$/well) into 6-wellplates. A straight scratch was introduced in HUVEC monolayers using a 200-μl plastic pipette tip. Following

incubation for a further 24 h in EBM containing 1% FBS, the average distance of the cells migrating into the wound was monitored by a light microscope (magnification, x100; Olympus Corporation). The migrated distance was calculated using ImageJ software (version1.49p; National Institutes of Health).

Transwell assay. Transwell inserts (Corning, Inc.) with a pore size of 8-μm were used to assess the migratory ability of ECs. HUVECs ($1x10^5$/well) were resuspended in 500 μl serum-free medium with SIN (30 μM) and subsequently added to the upper plate compartment. The medium supplemented with 10% FBS was filled to the bottom chamber. The invaded cells were treated with 4% paraformaldehyde for 10 min and stained with 0.1% crystal violet (Invitrogen; Thermo Fisher Scientific, Inc.) for 30 min at room temperature. Finally, the cells numbers in five randomly selected fields were counted under an inverted microscope (magnification, x100; Olympus Corporation).

Angiogenesis assay. For this assay, 96-well plates were pre-coated with Matrigel (50 μl) for 30 min at 37˚C. SIN was dissolved in DMSO, which was used as a control group. HUVECs were resuspended at $1\text{-}2x10^4$ cells/ml in serum-free EBM-2 with SIN and loaded on top of the Matrigel. Following culture for 6 h, the images were captured using a light microscope (magnification, x40; Olympus Corporation). Vessel morphometric parameters, including vessel number, were quantified using ImageJ software (version1.49p; National Institutes of Health). Tube formation was expressed as a percentage of the control group.

Western blotting. The lysates of HUVECs were extracted using RIPA lysis buffer. The homogenates were centrifuged at 12,000 x g for 15 min at 4˚C. The concentration levels of the protein samples were evaluated using a bicinchoninic acid protein analysis kit (Thermo Fisher Scientific, Inc.). Total protein (30 μg) was electrophoresed on 7.5 and 10% SDS-PAGE gels for 1 h using an electrophoresis apparatus (Bio-Rad Laboratories, Inc.) and transferred to PVDF membranes (MilliporeSigma) at 280 mA for 2 h, followed by blocking in 5% non-fat milk for 1.5 h. The membranes were incubated at 4˚C overnight with rabbit CD31, p-VEGFR2, VEGFR2, p-AKT, AKT, β-actin and GAPDH (1:1,000 each), HIF-1α (1:500), α-tubulin (1:3,000) and mouse VEGF (1:1,000) antibodies. Following washing with TBS-T (0.1% Tween-20) three times, the membranes were incubated with HRP-conjugated secondary antibodies (ShanghaiMorui Biotechnology) for 2 h at room temperature and developed with enhanced chemiluminescence (ECL; MilliporeSigma) reagents. The signal intensity was calculated using ImageJ software (version1.44p; National Institutes of Health).

Tumor-conditioned medium (CM) preparation. HepG2/C3A cells were plated at a density of $5x10^5$ cells/ml in 6-well plates with DMEM containing 10% FBS overnight. At 90% confluence, the cells were transferred from a normoxic (21% O_2) to a hypoxic (1% O_2) environment for 48 h following replacement of the medium with or without 30 μM SIN. The collected CM was filtered through a 0.2-μm filter (Corning, Inc.) and stored in a freezer at -80˚C.

ELISA of conditioned media. VEGF levels in HepG2/C3A CM were assessed using a human VEGF Quantikine ELISA kit (cat. no. E-TSEL-H0026; ELabscience Biotechnology, Inc.) following the manufacturer's protocol. The experiment was repeated in triplicate, with five biological samples each time.

Reverse transcription-quantitative (RT-q) PCR. HepG2/C3A cells ($2x10^5$/ml) were treated with or without SIN in 6-well plates under hypoxic conditions for 48 h. Total RNA in the cells was extracted using RNAiso Plus kit (Takara Bio, Inc.). The RNA concentration levels were measured using spectrophotometry (NanoDrop 2000; Thermo Fisher Scientific, Inc.). Following treatment with DNAse, 1 μg RNA was reverse-transcribed using a reverse transcriptase kit (Thermo Fisher Scientific, Inc.). RT-qPCR was performed using SYBR-Green I Master (Vazyme Biotech Co., Ltd.). RNA extraction, cDNA synthesis and qPCR were performed according to the manufacturer's protocols. The primer sequences used were obtained from a previously published study (22) and synthesized by Invitrogen (Thermo Fisher Scientific, Inc.). The thermocycling conditions were as follows: 95˚C for 30 sec, followed by 40 cycles at 95˚C for 10 sec and 60˚C for 30 sec. The relative expression levels of the target genes were normalized to that of GAPDH using the $2^{-\Delta\Delta Cq}$ method (23). The primer sequences used were: Human VEGF, forward, 5'-AAAGGGAAAGGGGCAAAAACG AA-3' and reverse, 5'-AGGAACATTTACACGTCTGCGG-3'; and human GAPDH, forward, 5'-TGATGACATCAAGAA GGTGGTGAAG-3' and reverse, 5'-TCCTTGGAGGCCATG TGGGCCAT-3'. All PCR was repeated in triplicate.

Molecular docking. The crystal structure file of VEGFR2 (PDB ID: 3VHE) was downloaded from the Protein Data Bank (PDB) database (http://www.rcsb.org/). Prior to docking, the water molecules of VEGFR2 were removed and subsequently hydrogen atoms and charges (24) were added to the structure of this receptor. The SIN structure file was obtained from the following website: http://zinc.docking.org/. Molecular docking was used to predict the optimal binding site for SIN to VEGFR2 (AutoDock 4.2) (25). The docking position of SIN on VEGFR2 was defined at the active site with a proper grid box; the grid box size was 68x72x74; the grid center was -24.402 Å, -0.107 Å and -4.276 Å and the grid space was 0.704 Å. The optimal binding mode between SIN and VEGFR2 was acquired under the minimum binding free energy conformation and the output results of AutoDock 4.2 were presented to PyMol 1.8.2.0 (Schrödinger, LLC) and Discovery Studio 2016 Client (BIOVIA Discovery Studio Client v16; Dassault Systèmes) software for further analysis.

Statistical analysis. All results are presented as the mean ± standard deviation (SD). Unpaired Student's t-test was applied for two-group comparisons. Significance among multiple groups were calculated by one-way ANOVA with Bonferroni's post-hoc test using GraphPad Prism 5 (GraphPad Software, Inc.). $P<0.05$ was considered to indicate a statistically significant difference.

Results

SIN inhibited the growth and angiogenesis of HepG2/C3A-derived tumors in vivo. The chemical structure

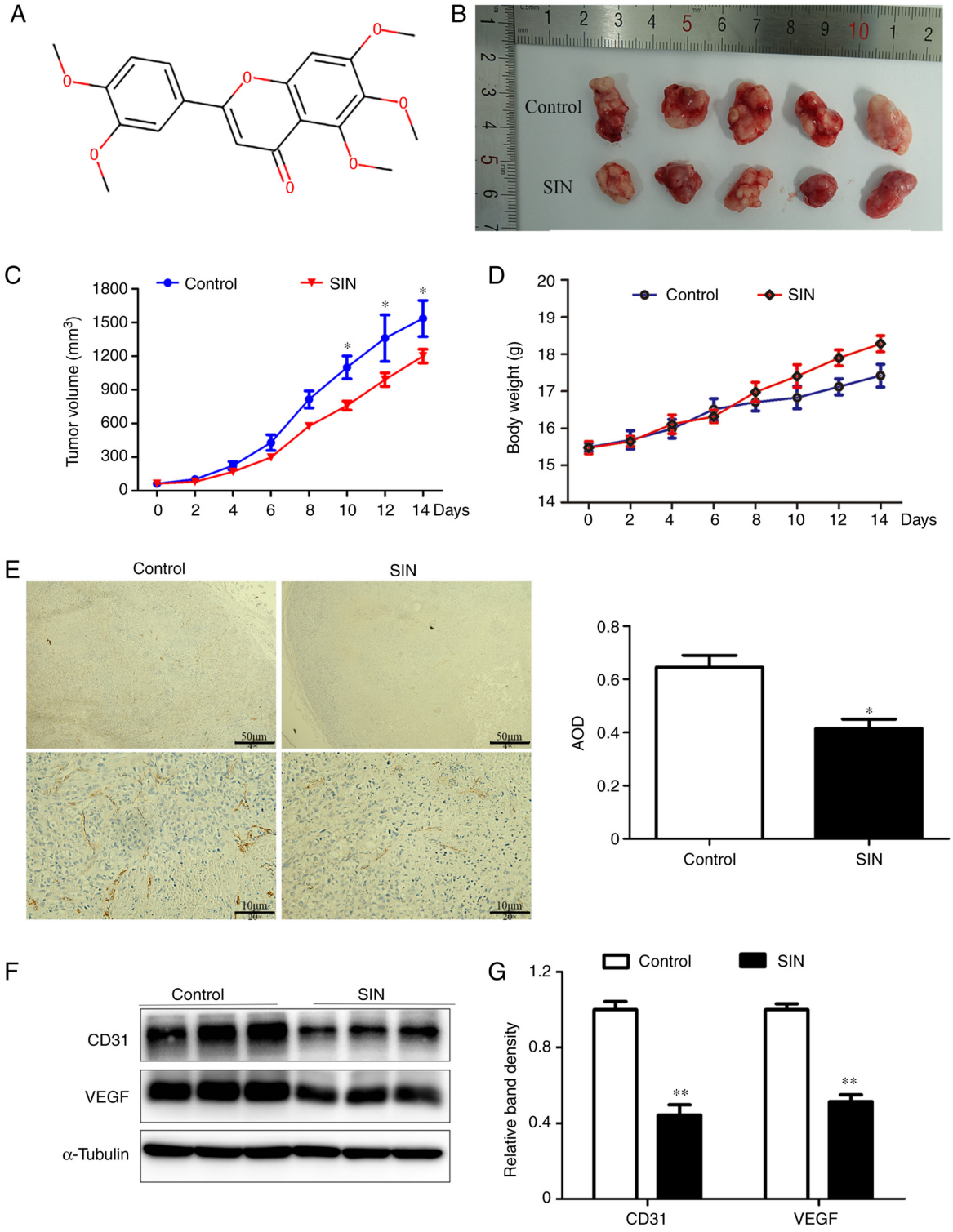

Figure 1. Effects of SIN on HepG2/C3A tumor growth and angiogenesis in BALB/c nude mice. (A) Chemical structure of SIN. (B) Representative images of HepG2/C3A cell-derived tumors obtained on the last day of the animal experiment. (C) Growth curve of HepG2/C3A cell-derived tumors. n=5, *P<0.05 vs. the control group. (D) Body weight change of the different groups. n=5. (E) Representative images of IHC staining (magnification, x200) in tumor samples on day 14 and statistical analysis of CD31 staining results. n=3, *P<0.05 vs. the control group. (F and G) Western blotting and relative gray value analyses of CD31 and VEGF protein expressions in tumor tissues. n=3, **P<0.01. SIN, sinensetin; IHC, immunohistochemical; CD31, platelet/endothelial cell adhesion molecule-1; VEGF, vascular endothelial growth factor; AOD, average optical density.

of SIN is displayed in Fig. 1A. To examine whether SIN could inhibit tumor growth *in vivo*, HepG2/C3A tumor models were established in BALB/c nude mice. The analysis of the growth curve of model mice indicated that SIN exerted an antitumor effect. As depicted in Fig. 1B, after 14 days of treatment with SIN or saline, the tumor volume in SIN treatment group was smaller than the control group. The difference became more significant with increasing the drug application time (Fig. 1C) (day 10, 12 and 14; P<0.05). As one of cachexia-associated symptoms, the body weight of control group increased slowly,

but there were no significant differences between the two groups (Fig. 1D). As CD31 is a marker of neovascularization (26), CD31expression was evaluated using IHC analysis and western blotting. Staining for CD31 revealed that CD31 expression was significantly lower in SIN treatment group than in the control group (Fig. 1E; P<0.05). The CD31 results of western blotting were also lower in SIN group, consistent with the results of IHC staining (Fig. 1F and G; P<0.01). As an indicator of growing tumor tissue, VEGF could promote the growth of ECs (15). Western blotting revealed that SIN inhibited VEGF expression in HepG2/C3A-derived tumor tissues (Fig. 1F and G).

SIN suppresses angiogenesis in vitro by promoting apoptosis and inhibiting proliferation, migration and tube formation of HUVECs. Under different SIN concentrations (3, 10, 30, 60 and 100 μM) for 24 h, cytotoxicity was measured using CCK8 assay. VEGF was used as a positive control in the present study. As an angiogenic factor secreted by tumor cells under hypoxic conditions (15), VEGF will bind to VEGF receptor 2 on ECs (27) and promote proliferation, migration and survival of ECs. As shown in Fig. 2A, SIN demonstrated a concentration-dependent inhibitory effect on the proliferation of HUVEC. In addition, endothelial cell proliferation induced by VEGF can be inhibited by SIN. These results suggested that SIN inhibited the proliferation of HUVEC. For 30, 60 and 100 μM, this effect was significant (P<0.01). Hence, SIN at a concentration of 30 μM was employed for subsequent experiments. To further explore the reasons for decreased cell viability, the apoptosis levels of HUVECs were assessed by Annexin V-FITC/PI stain. DMSO-dissolved SIN (30 μM) was added to the experimental group. Flow cytometry results revealed that VEGF inhibited apoptosis in HUVECs, but it was reversed by SIN (Fig. 2B; P<0.01). As wound healing assays and Transwell assays showed, HUVEC migration was enhanced by VEGF compared to the control group but was significantly attenuated in SIN-treatment group (P<0.05; Fig. 2C; P<0.01; Fig. 2D). To further explore the potential antiangiogenic effect of SIN, tube formation was performed in 96-well plates. The experimental results indicated that VEGF could promote tube formation; by contrast, SIN inhibited angiogenesis *in vitro* (P<0.01; Fig. 2E). The migration assays and tube formation also showed a decreased tendency in SIN group compared to control group, but were not statistically significant. All these data indicated that angiogenesis was suppressed by SIN.

SIN suppresses angiogenesis by inhibiting the activity of VEGF in HepG2/C3A. VEGF is a pivotal enabling factor for angiogenesis (28), which HIF regulates (29). HIF-1α, as a regulatory subunit, can be increased under hypoxic conditions (30). HepG2/C3Acells were exposed to 30 μM SIN under hypoxic conditions for 48 h and western blot analyses revealed that HIF-1α and VEGF levels were significantly elevated under hypoxic conditions (P<0.05) but could be reversed by SIN (P<0.05; Fig. 3A). After incubation with SIN (30 μM) under hypoxic conditions for 48 h, CM of HepG2/C3A was collected to detect the secretion level of VEGF in the supernatant. The results revealed that VEGF content in CM increased significantly under hypoxia (P<0.001), but was inhibited under SIN treatment (P<0.05; Fig. 3B). VEGF mRNA expression was measured in SIN-treated HepG2/C3A cells under hypoxic conditions and PCR results revealed that SIN demonstrated a robust VEGF inhibitory effect under hypoxic conditions (P<0.05; Fig. 3C). As one of the tumor cell-secreted angiogenic growth factors, VEGF is a crucial agent for angiogenesis (31). To mimic *in vivo* angiogenesis events, CM of HepG2/C3A cells were collected to coculture with HUVECs (32) after 48 h of hypoxia exposure in a serum-free medium. CM from non-SIN-treated HepG2/C3A cells was used as the control. Tube formation was observed after 6 h CM treatment. As shown in Fig. 3D, hypoxia increased VEGF and promoted angiogenesis, but SIN repressed VEGF expression and inhibited angiogenesis (P<0.001). These results indicated that the decrease of VEGF induced by SIN in HepG2/C3A cells contributed to angiogenesis inhibition.

SIN inhibits phosphorylation of VEGFR2 and AKT signaling pathway. VEGF binds to VEGF receptor 2 on ECs and promotes proliferation, migration and survival of ECs (33). To explicit the effect of SIN on VEGFR2 protein expression, HUVECs were treated with SIN containing exogenous VEGF or not for 30 min and then western blotting performed. p-AKT, as a downstream signaling molecule of p-VEGFR2, was also observed by western blotting. Phosphorylation levels of VEGFR2 and AKT were significantly increased under VEGF treatment (both P<0.01), while they were decreased in SIN-treated HUVEC, even with VEGF (both P<0.05; Fig. 4A and B).

To further demonstrate the anti-angiogenesis mechanism of SIN, whether it depended on p-VEGFR2, p-AKT, or both, VEGF and SU1498 were used in a serum-free medium to treat HUVECs. As a selective inhibitor of VEGFR2, SU1498 was used as a positive control (34). Immunoblot analyses revealed that phosphorylation of VEGFR2 was inhibited by SIN similarly to SU1498 (Fig. 5A). IGF-1, which is an activator of PI3K/AKT pathway, was used as a negative control (35). AKT is a downstream target protein of VEGFR2 (36). After 90 min exposure to IGF (10 ng/ml), AKT phosphorylation in HUVECs significantly increased, but it could not be reversed by SIN (Fig. 5B). The above results suggested that SIN mainly acted on VEGFR2 to inhibit angiogenesis rather than acted directly on AKT.

Molecule docking analysis. As one of the best theoretical methods, molecular docking has traditionally been employed to study binding affinities between target proteins and virtually screened ligands (37). To more effectively mimic the internal environment, molecular docking analysis was performed using VEGFR2 (PDB ID: 3VHE) to determine the interactions between SIN and VEGFR2 (38). Molecular docking studies revealed that SIN occupied the active site, as displayed in Fig. 6A-C. SIN was surrounded by some hydrophobic residues (PHE918, VAL899, VAL916, LEU840, GLY922, ALA866, LEU1035, PHE1047, VAL848 and ALA1050) and some polar residues (CYS919, GLU917, LYS868, ASN923, CYS1045 and LYS920), as depicted in Fig. 6D. The hydrophobic force may contribute to the interactions between SIN and VEGFR2. The hydrogen bond interactions between SIN and CYS 919 residue might decrease the hydrophilicity while increasing the hydrophobicity of VEGFR 2. As demonstrated

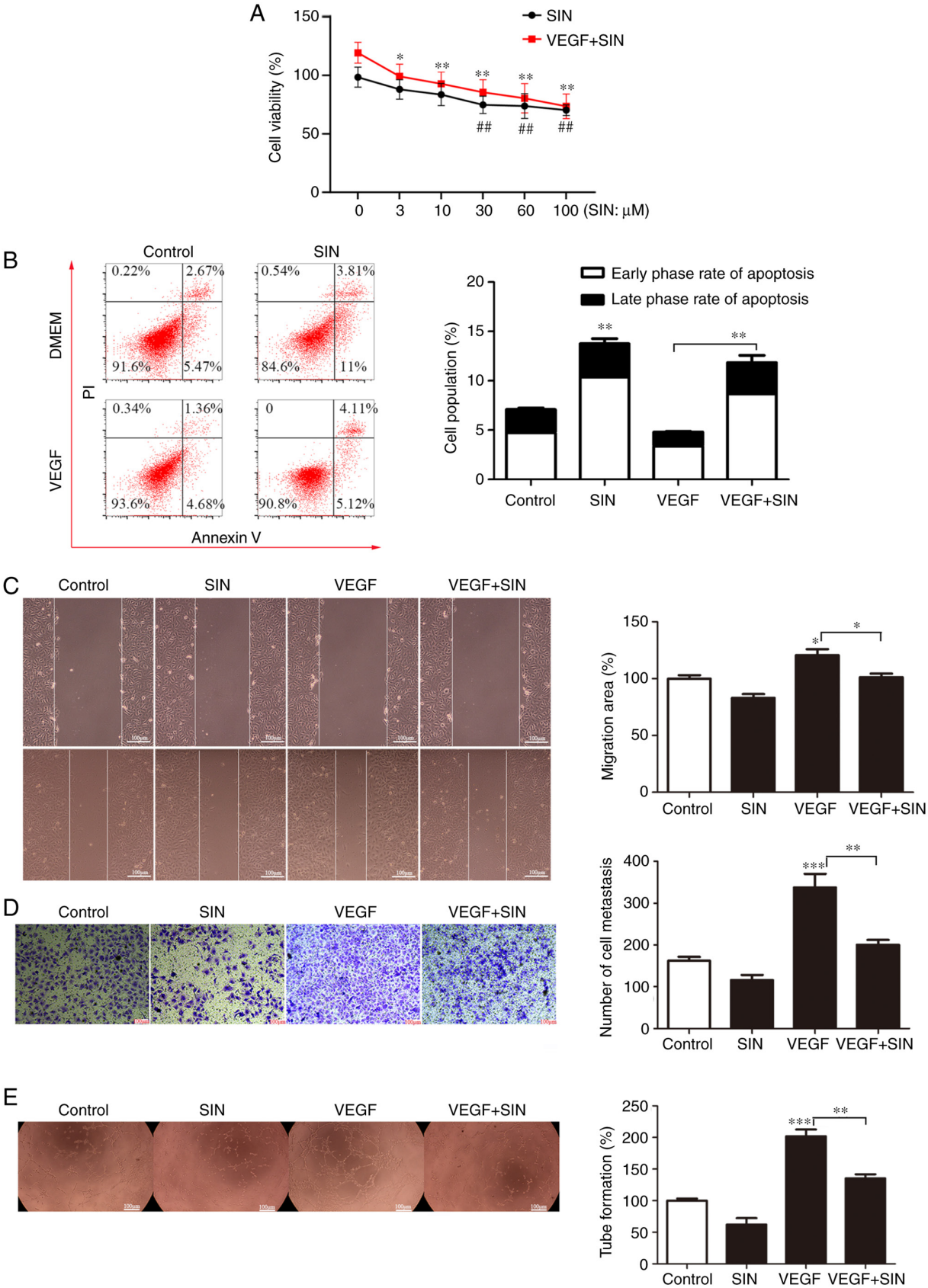

Figure 2. SIN inhibits angiogenesis *in vitro* by promoting apoptosis and inhibiting HUVEC migration, proliferation and tube formation. (A) Inhibitory effects of different doses of SIN on the proliferation of HUVECs. The data are presented as percentages of respective control values for cell viability. n=8, *P<0.05, **P<0.01, VEGF + SIN group vs. the VEGF + vehicle group; $^{\#\#}$P<0.01, SIN group vs. the vehicle group. (B) Effects of SIN on induction of HUVEC apoptosis. The cells were treated with or without VEGF and SIN. The levels of apoptosis were assessed using flow cytometry analysis. n=3, **P<0.01. (C) The effects of SIN on the migration of HUVECs were assessed using the wound-healing assay (magnification, x100). n=3, *P<0.05. (D) SIN inhibits HUVEC migration as demonstrated by Transwell assays (magnification, x100). n=3, **P<0.01, ***P<0.001. (E) The angiogenic activity of HUVECs was inhibited by SIN as determined by the tube formation assays (magnification, x40). n=8, **P<0.01, ***P<0.001. SIN, sinensetin; HUVEC, human umbilical vein endothelial cells; VEGF, vascular endothelial growth factor.

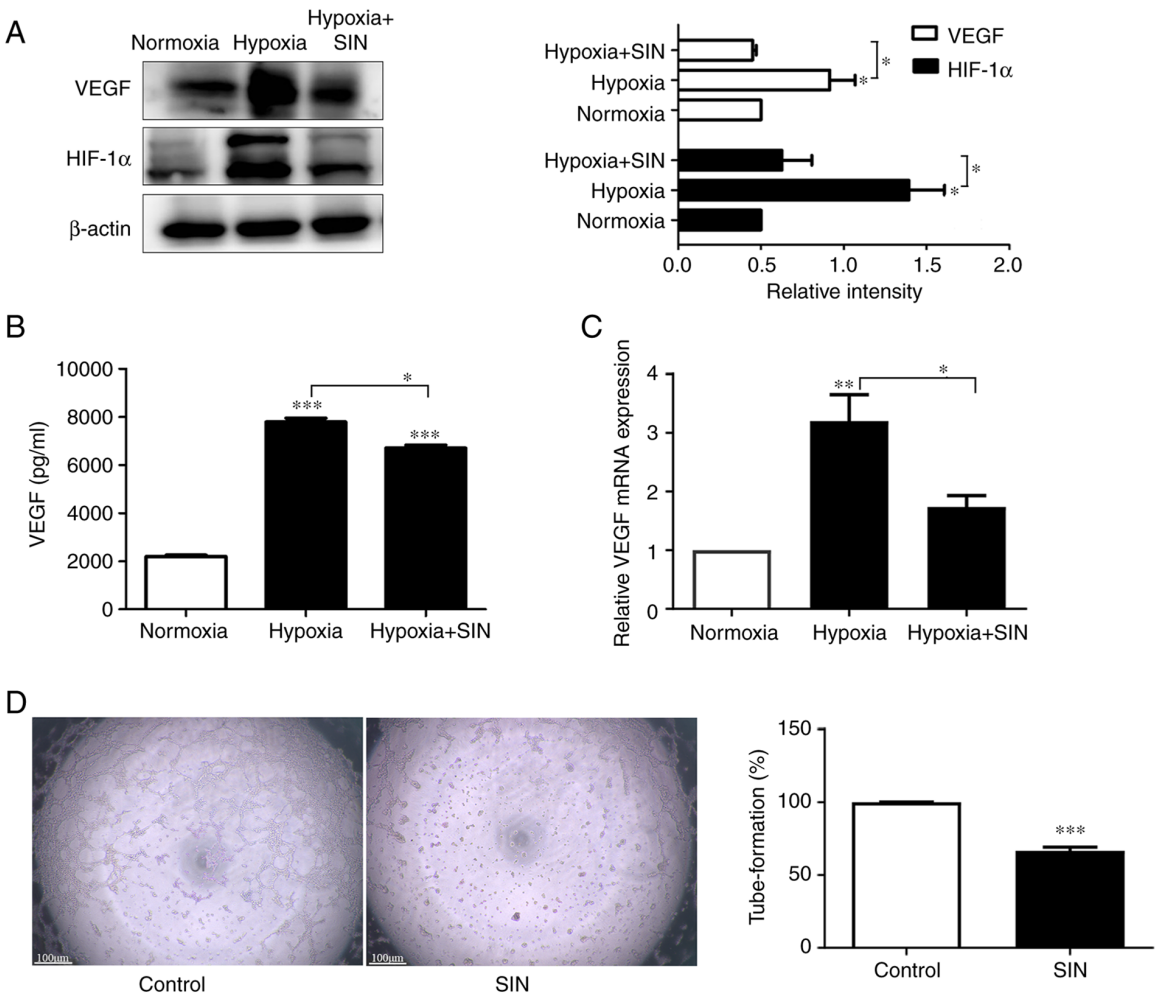

Figure 3. SIN suppresses angiogenesis by inhibiting the activity of VEGF in HepG2/C3A cells. (A) SIN down regulated the expression levels of VEGF and HIF-1α under hypoxic conditions as determined by western blot analysis. n=3, *P<0.05. (B) SIN inhibits VEGF secretion of HepG2/C3A cells under hypoxic conditions as determined by ELISA. n=5, *P<0.05, ***P<0.001. (C) The expression levels of VEGF were analyzed by RT-qPCR in HepG2/C3A cells. n=3, *P<0.05, **P<0.01. (D) HepG2/C3A cells were pre-incubated with SIN for 48 h in a hypoxic environment and subsequently CM was collected to assess tube formation. SIN-treated CM inhibits the tube-formation ability of HUVEC (magnification, x40). n=8, ***P<0.001. SIN, sinensetin; VEGF, vascular endothelial growth factor; HIF-1α, hypoxia-inducible factor 1α; RT-qPCR, reverse transcription-quantitative PCR; CM, tumor-conditioned medium.

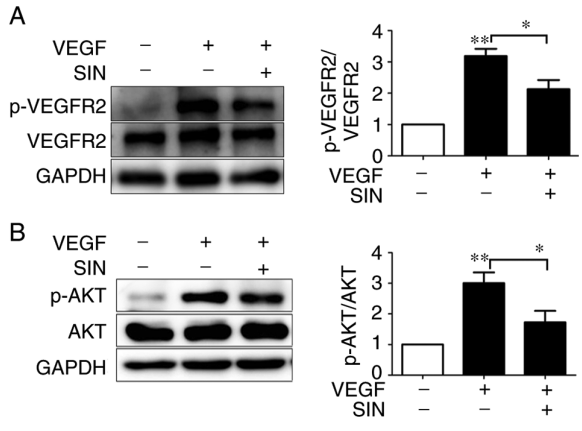

Figure 4. SIN inhibits phosphorylation of VEGFR2 and AKT in HUVECs. (A) SIN inhibits the phosphorylation of VEGFR2 induced by VEGF. The expression levels of p-VEGFR2 and VEGFR2 in HUVECs treated with SIN were analyzed by western blotting. n=3, *P<0.05, **P<0.01. (B) SIN inhibited VEGFR2-induced phosphorylation of AKT. p-AKT and AKT were examined in HUVECs following treatment with SIN. n=3, *P<0.05, **P<0.01. SIN, sinensetin; VEGFR, vascular endothelial growth factor receptor; HUVECs, human umbilical vein endothelial cells; VEGF, vascular endothelial growth factor; p-, phosphorylated.

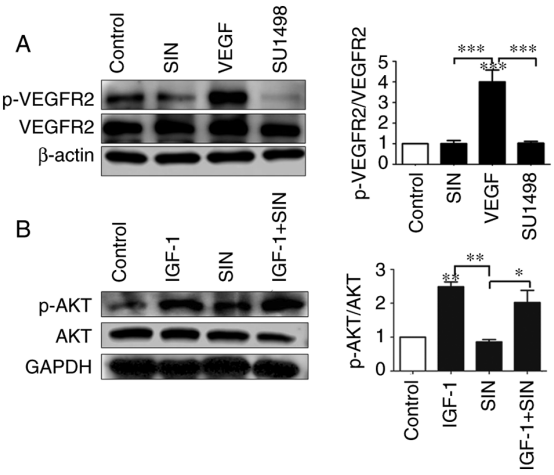

Figure 5. Decrease in AKT phosphorylation levels induced by SIN is dependent on the decrease of VEGFR2 phosphorylation. (A) The inhibitory effect of SIN on VEGFR2 phosphorylation was similar to that of SU1498. n=3, ***P<0.001. (B) SIN inhibits VEGFR2-induced phosphorylation of AKT, which is reversible by IGF-1. n=3, *P<0.05, **P<0.01. SIN, sinensetin; VEGFR, vascular endothelial growth factor receptor; IGF-1, insulin-like growth factor 1.

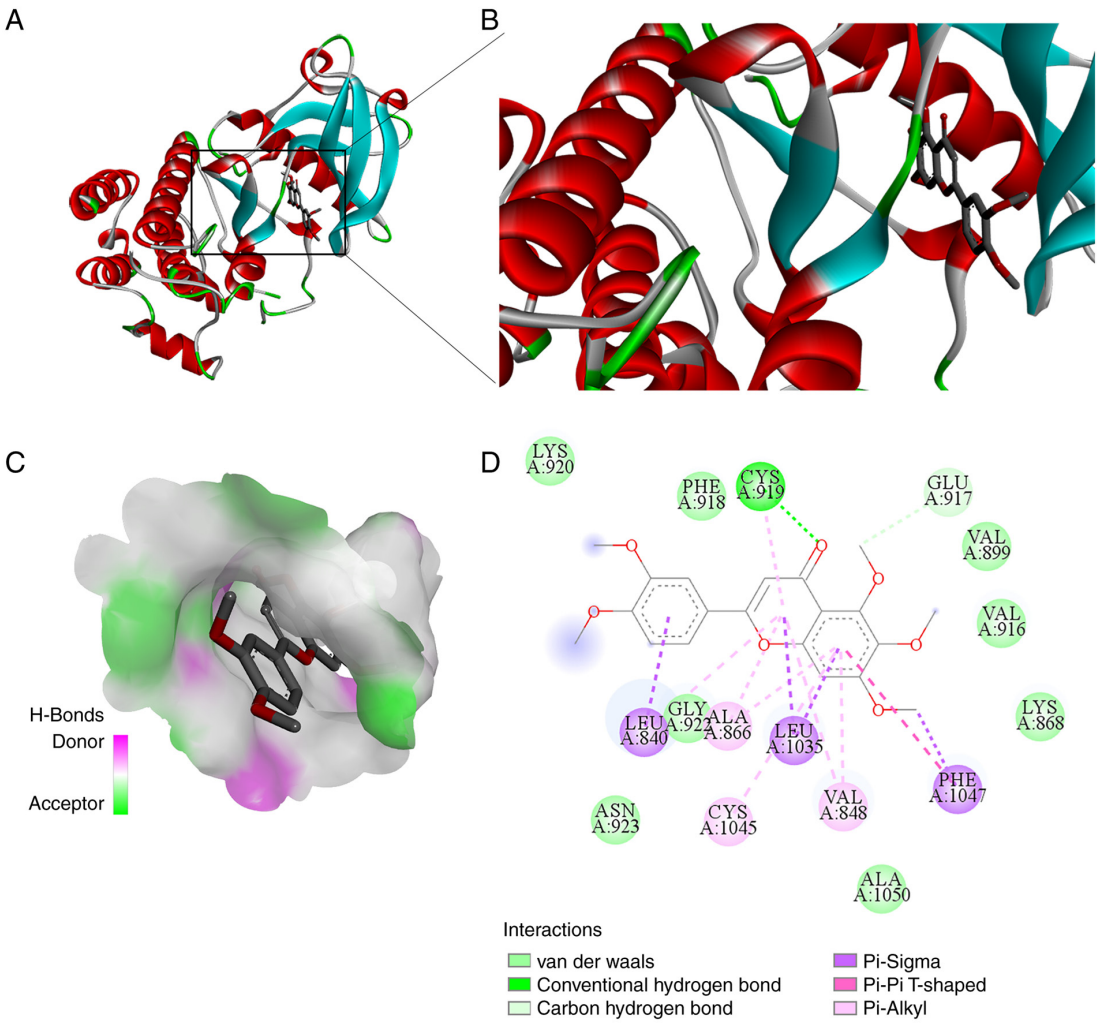

Figure 6. Optimal conformations between SIN and VEGFR2 are estimated by molecular docking. (A) The binding modes of the SIN-VEGFR2 complex with minimum energy. (B) The overall interactions between SIN and the protein residues. (C) The optimal binding position of SIN with VEGFR2. (D) Representation of the interaction between SIN and VEGFR2. SIN, sinensetin; VEGFR, vascular endothelial growth factor receptor.

in Fig. 6D, the residue GLU917held SIN at the active site through carbon-hydrogen bonds. The residue PHE1047 formed a π-π T-shaped interaction, ALA866, CYS1045 and VAL848 combined with SIN through π-alkyl interactions. Furthermore, the residues LEU840, LEU1035 and PHE1047 held SIN at the binding pocket via π-Sigma interactions. Additionally, the residues LYS920, PHE918, VAL899, VAL916, LYS868, GLY922, ASN923 and ALA1050 formed van der Waals forces between the pocket and SIN. These results indicate that SIN inactivates the VEGF/VEGFR2 axis, resulting in decreased AKT phosphorylation downstream and participating in its anti-angiogenesis effect (Fig. 7).

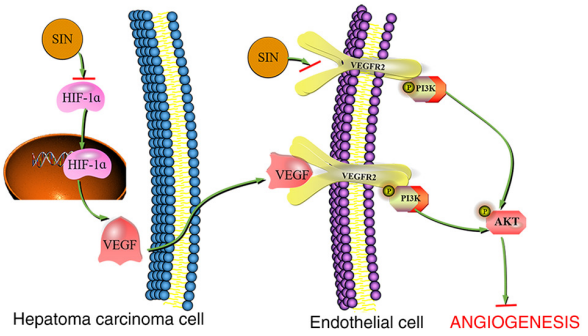

Figure 7. Schematic diagram summarizing the signaling pathway by which SIN inhibits liver cancer angiogenesis. SIN represses VEGF expression by downregulating HIF-1α expression. SIN inhibits VEGF-induced VEGFR2 phosphorylation and sequentially inhibits the levels of p-AKT leading to inhibition of EC proliferation, migration, tube formation and angiogenesis. SIN, sinensetin; VEGF, vascular endothelial growth factor; HIF, hypoxia-inducible factors; VEGFR, vascular endothelial growth factor receptor; EC, endothelial cell; p, phosphorylated.

Discussion

Chinese herbs are an essential part of Traditional Chinese Medicine and contribute to liver cancer management in China (39). *Fructus Aurantii Immaturus* is frequently used in Traditional Chinese Medicine and is rich in flavonoids that exhibit multiple biological effects, including anticancer activity in human liver cancer (40). SIN is a methoxyflavone commonly found in citrus species, exhibiting an anticancer effect on liver cancer (10,41). Tumor growth depends on angiogenesis to provide nutrition and oxygen to tumor cells (42). Although SIN has been shown to promote autophagy-related hepatocellular carcinoma cell death, the

impact of this compound on angiogenesis of liver cancer has not been confirmed.

In the present study, an *in vivo* animal model study was used to indicate that SIN restrained HepG2/C3A-derived tumor growth. A previous study (43) demonstrated that CD31 is enriched at the EC intercellular junctions; this receptor is considered a neoangiogenesis marker. IHC staining and western blot analysis of CD31 revealed that SIN inhibited CD31 expression in tumor tissues, suggesting that this compound exhibited an antiangiogenic effect in liver cancer *in vivo*. Western blot analysis indicated that SIN reduced VEGF secretion in tumor cells; this may be the mechanism responsible for the suppression of tumor angiogenesis caused by SIN.

Angiogenesis requires EC proliferation and migration to appropriate positions leading to their assembly in vascular structures (44). Therefore, the present study investigated the antiangiogenic effect of SIN *in vitro*. SIN exhibited significant cytotoxicity to HUVECs even in the presence of VEGF, which was consistent with the study of Lam *et al* (45). VEGF is a potent regulator of angiogenesis that inhibits the induction of EC apoptosis in new blood vessels (46). Subsequently, the induction of apoptosis by SIN was evaluated. Flow cytometry results demonstrated that induction of HUVEC apoptosis was maintained at a low level in the presence of VEGF compared with that of the normal group, whereas it was increased following treatment of the cells with SIN. Angiogenesis relies on EC destabilization, dissociation and migration. The present study revealed that SIN may delay HUVEC migration, as determined by the wound healing results. The results of the tube formation assays indicated that SIN could inhibit the angiogenic activity of ECs induced by VEGF. Based on these results, SIN was shown to inhibit angiogenesis, albeit with an unknown mechanism.

Angiogenesis is necessary for tumor development and provides oxygen and nutrients to tumor cells (47). Circulating VEGF levels are increased in hepatocellular carcinoma and are linked to tumor angiogenesis and progression (48). VEGF is a mitogen of ECs that promotes their proliferation and migration into tumors required for the formation of new capillaries (49). Western blot analysis revealed that HepG2/C3A-derived VEGF was reduced by SIN. Due to the rapid growth of tumor cells leading to hypoxia, the expression levels of HIF increase, causing VEGF upregulation and promoting angiogenesis (29). SIN treatment was accompanied by reduced protein levels of HIF-1α, which may mediate VEGF downregulation induced by SIN. To further account for these phenomena, a tube formation experiment was used to assess whether SIN inhibits angiogenesis via the HIF-1α-VEGF pathway.

VEGF binds to VEGFR2 on the EC membrane and initiates angiogenesis (33). Subsequently, VEGFR2 is phosphorylated and activates the downstream intracellular pathway, which promotes the proliferation, migration and survival of ECs (50). The present study demonstrated that SIN downregulated VEGFR2 phosphorylation. The data indicated that VEGFR2 phosphorylation in HUVECs was increased following addition of VEGF for 30 min; however, this increase was eliminated with the addition of SIN. When SIN was replaced by SU1498, a specific inhibitor of VEGFR2 (51), the same results were observed. In VEGF-induced conditions, SIN specifically suppressed the phosphorylation of VEGFR2, while this effect was not noted in the SIN group in the absence of VEGF. This may explain why the SIN-treated group did not differ significantly from the control group with regard to tube formation and migratory activity.

VEGFR2 phosphorylation activates downstream signaling pathways, such as MAPK/ERK and PI3K/AKT (36). Western blot analysis indicated that the phosphorylation levels of ERK in HUVECs did not change significantly following SIN treatment, suggesting that SIN-induced inhibition of angiogenesis was independent of the MAPK/ERK pathway. However, SIN downregulated the phosphorylation levels of AKT in VEGF-treated cells. To further confirm that inhibition of SIN-induced angiogenesis relies on the VEGFR2/AKT pathway, IGF-1, which is an activator of the PI3K/AKT pathway, was added prior to SIN treatment. Western blot analysis demonstrated that SIN did not reverse IGF-1-induced phosphorylation of AKT. Furthermore, the binding of SIN to VEGFR2 was simulated using molecular docking. The molecular docking data suggested that SIN directly interacted with VEGFR2 by various important residues, confirming that this compound could directly bind to VEGFR2 and produce antiangiogenic effects. Therefore, the VEGF/VEGFR2/AKT pathway may be the mechanism by which SIN inhibits liver cancer angiogenesis.

The current study contains certain limitations. Although it was shown that the expression levels of the HIF-1α protein were downregulated by SIN, the detailed mechanism of this process remains unclear. The translation of the HIF-1α protein is considered to be an important regulatory mechanism of HIF-1α-inhibiting compounds (52). Therefore, further studies are required to explore the mechanisms that are related to the protein translation of HIF-1α.

In summary, the present study demonstrated that SIN exhibited a significant antiangiogenic effect by inhibiting the viability of ECs and inducing apoptosis. Concomitantly, SIN suppressed angiogenesis by inhibiting the migratory activity and tube formation in HUVECs. SIN potently inhibited angiogenesis *in vitro* by eliciting the blockade of VEGF expression in HepG2/C3A-derived tumors and the inhibition of the VEGFR2/AKT signaling pathway in ECs. The results of the present study may be necessary for developing strategies that aim to prevent liver cancer with SIN.

Acknowledgements

Not applicable.

Funding

The present study was financed in part by the Traditional Chinese Medicine Science and Technology Development Plan Project of Shandong Province, China (grant no. 2019-0370), the Natural Science Foundation of Shandong Province (grant nos. ZR2019BH007 and ZR2019MH128), Youth Science and Technology Innovation Team Projects of Higher Learning Institutions of Shandong Province, China (grant no. 2019KJK013) and Youth research and innovation team of Shandong University of Traditional Chinese Medicine, China (grant no. 17).

Availability of data and materials

The datasets used and/or analyzed during the current study are available from the corresponding author on reasonable request.

Authors' contributions

JLiu designed the experiments. XL, YLi and YWa performed the experiments and prepared the article. FL, YLiu, YWu, HR and XZ performed the animal experiments and analysis. JLia and RZ participated in data analysis discussions. XL and JLiu confirm the authenticity of all the raw data. All authors read and approved the final manuscript.

Ethics approval and consent to participate

All animal experiments and experimental protocols were approved by the Ethics Committee of Qianfoshan Hospital (Jinan, China; approval no. 2017-106; approval date: 14 December 2017).

Patient consent for publication

Not applicable.

Competing interests

The authors declare that they have no competing interests.

References

1. Carmeliet P and Jain RK: Principles and mechanisms of vessel normalization for cancer and other angiogenic diseases. Nat Rev Drug Discov 10: 417-427, 2011.
2. Carmeliet P: Angiogenesis in life, disease and medicine. Nature 438: 932-936, 2005.
3. Xue C, Shao S, Yan Y, Yang S, Bai S, Wu Y, Zhang J, Liu R, Ma H, Chai L, *et al*: Association between G-protein coupled receptor 4 expression and microvessel density, clinicopathological characteristics and survival in hepatocellular carcinoma. Oncol Lett 19: 2609-2620, 2020.
4. Welker MW and Trojan J: Anti-angiogenesis in hepatocellular carcinoma treatment: Current evidence and future perspectives. World J Gastroenterol 17: 3075-3081, 2011.
5. Edeline J, Boucher E, Rolland Y, Vauléon E, Pracht M, Perrin C, Le Roux C and Raoul JL: Comparison of tumor response by response evaluation criteria in solid tumors (RECIST) and modified RECIST in patients treated with sorafenib for hepatocellular carcinoma. Cancer 118: 147-156, 2012.
6. Zhang H, Tian G, Zhao C, Han Y, DiMarco-Crook C, Lu C, Bao Y, Li C, Xiao H and Zheng J: Characterization of polymethoxyflavone demethylation during drying processes of citrus peels. Food Funct 10: 5707-5717, 2019.
7. Huang B, Zhai M, Qin A, Wu J, Jiang X and Qiao Z: Sinensetin flavone exhibits potent anticancer activity against drug-resistant human gallbladder adenocarcinoma cells by targeting PTEN/PI3K/AKT signalling pathway, induces cellular apoptosis and inhibits cell migration and invasion. J BUON 25: 1251-1256, 2020.
8. Tan KT, Lin MX, Lin SC, Tung YT, Lin SH and Lin CC: Sinensetin induces apoptosis and autophagy in the treatment of human T-cell lymphoma. Anticancer Drugs 30: 485-494, 2019.
9. Dong Y, Ji G, Cao A, Shi J, Shi H, Xie J and Wu D: Effects of sinensetin on proliferation and apoptosis of human gastric cancer AGS cells. Zhongguo Zhong Yao Za Zhi 36: 790-794, 2011 (In Chinese).
10. Kim SM, Ha SE, Lee HJ, Rampogu S, Vetrivel P, Kim HH, Venkatarame Gowda Saralamma V, Lee KW and Kim GS: Sinensetin induces autophagic cell death through p53-related AMPK/mTOR signaling in hepatocellular carcinoma HepG2 cells. Nutrients 12: 2462, 2020.
11. Stevens M and Oltean S: Modulation of receptor tyrosine kinase activity through alternative splicing of ligands and receptors in the VEGF-A/VEGFR axis. Cells 8: 288, 2019.
12. Guo D, Wang Q, Li C, Wang Y and Chen X: VEGF stimulated the angiogenesis by promoting the mitochondrial functions. Oncotarget 8: 77020-77027, 2017.
13. Yan ZX, Luo Y and Liu NF: Blockade of angiopoietin-2/Tie2 signaling pathway specifically promotes inflammation-induced angiogenesis in mouse cornea. Int J Ophthalmol 10: 1187-1194, 2017.
14. Al-Aqtash RA, Zihlif MA, Hammad H, Nassar ZD, Meliti JA and Taha MO: Ligand-based computational modelling of platelet-derived growth factor beta receptor leading to new angiogenesis inhibitory leads. Comput Biol Chem 71: 170-179, 2017.
15. Shibuya M: Vascular endothelial growth factor (VEGF) and its receptor (VEGFR) signaling in angiogenesis: A crucial target for anti- and pro-angiogenic therapies. Genes Cancer 2: 1097-1105, 2011.
16. Li S, Xu G, Gao F, Bi J and Huo R: Expression and association of VEGF-Notch pathways in infantile hemangiomas. Exp Ther Med 14: 3737-3743, 2017.
17. Dulloo I, Phang BH, Othman R, Tan SY, Vijayaraghavan A, Goh LK, Martin-Lopez M, Marques MM, Li CW, Wang de Y, *et al*: Hypoxia-inducible TAp73 supports tumorigenesis by regulating the angiogenic transcriptome. Nat Cell Biol 17: 511-523, 2015.
18. Schlieve CR, Mojica SG, Holoyda KA, Hou X, Fowler KL and Grikscheit TC: Vascular endothelial growth factor (VEGF) bioavailability regulates angiogenesis and intestinal stem and progenitor cell proliferation during postnatal small intestinal development. PLoS One 11: e0151396, 2016.
19. Nicolas S, Abdellatef S, Haddad MA, Fakhoury I and El-Sibai M: Hypoxia and EGF stimulation regulate VEGF expression in human glioblastoma multiforme (GBM) cells by differential regulation of the PI3K/Rho-GTPase and MAPK pathways. Cells 8: 1397, 2019.
20. Tang Q, He X, Liao H, He L, Wang Y, Zhou D, Ye S and Chen Q: Ultrasound microbubble contrast agent-mediated suicide gene transfection in the treatment of hepatic cancer. Oncol Lett 4: 970-972, 2012.
21. Xiong YJ, Deng ZB, Liu JN, Qiu JJ, Guo L, Feng PP, Sui JR, Chen DP and Guo HS: Enhancement of epithelial cell autophagy induced by sinensetin alleviates epithelial barrier dysfunction in colitis. Pharmacol Res 148: 104461, 2019.
22. Liu F, Wang B, Li L, Dong F, Chen X, Li Y, Dong X, Wada Y, Kapron CM and Liu J: Low-dose cadmium upregulates VEGF expression in lung adenocarcinoma cells. Int J Environ Res Public Health 12: 10508-10521, 2015.
23. Livak KJ and Schmittgen TD: Analysis of relative gene expression data using real-time quantitative PCR and the 2(-Delta Delta C(T)) method. Methods 25: 402-408, 2001.
24. Wang R, Liu Y, Hu X, Pan J, Gong D and Zhang G: New insights into the binding mechanism between osthole and β-lactoglobulin: Spectroscopic, chemometrics and docking studies. Food Res Int 120: 226-234, 2019.
25. Cao X, Wang S, Bi R, Tian S, Huo Y and Liu J: Toxic effects of Cr(VI) on the bovine hemoglobin and human vascular endothelial cells: Molecular interaction and cell damage. Chemosphere 222: 355-363, 2019.
26. Okamura S, Osaki T, Nishimura K, Ohsaki H, Shintani M, Matsuoka H, Maeda K, Shiogama K, Itoh T and Kamoshida S: Thymidine kinase-1/CD31 double immunostaining for identifying activated tumor vessels. Biotech Histochem 94: 60-64, 2019.
27. Holmqvist K, Cross MJ, Rolny C, Hägerkvist R, Rahimi N, Matsumoto T, Claesson-Welsh L and Welsh M: The adaptor protein shb binds to tyrosine 1175 in vascular endothelial growth factor (VEGF) receptor-2 and regulates VEGF-dependent cellular migration. J Biol Chem 279: 22267-22275, 2004.
28. Farhat FS, Tfayli A, Fakhruddin N, Mahfouz R, Otrock ZK, Alameddine RS, Awada AH and Shamseddine A: Expression, prognostic and predictive impact of VEGF and bFGF in non-small cell lung cancer. Crit Rev Oncol Hematol 84: 149-160, 2012.

29. Forsythe JA, Jiang BH, Iyer NV, Agani F, Leung SW, Koos RD and Semenza GL: Activation of vascular endothelial growth factor gene transcription by hypoxia-inducible factor 1. Mol Cell Biol 16: 4604-4613, 1996.
30. Semenza GL, Agani F, Booth G, Forsythe J, Iyer N, Jiang BH, Leung S, Roe R, Wiener C and Yu A: Structural and functional analysis of hypoxia-inducible factor 1. Kidney Int 51: 553-555, 1997.
31. Ye J and Yuan L: Inhibition of p38 MAPK reduces tumor conditioned medium-induced angiogenesis in co-cultured human umbilical vein endothelial cells and fibroblasts. Biosci Biotechno lBiochem 71: 1162-1169, 2007.
32. Liu J, Yuan L, Molema G, Regan E, Janes L, Beeler D, Spokes KC, Okada Y, Minami T, Oettgen P and Aird WC: Vascular bed-specific regulation of the von Willebrand factor promoter in the heart and skeletal muscle. Blood 117: 342-351, 2011.
33. Shibuya M: Structure and function of VEGF/VEGF-receptor system involved in angiogenesis. Cell Struct Funct 26: 25-35, 2001.
34. Shu-Ya T, Qiu-Yang Z, Jing-Jing L, Jin Y and Biao Y: Suppression of pathological ocular neovascularization by a small molecule, SU1498. Biomed Pharmacother 128: 110248, 2020.
35. Chen S, Hu M, Shen M, Wang S, Wang C, Chen F, Tang Y, Wang X, Zeng H, Chen M, *et al*: IGF-1 facilitates thrombopoiesis primarily through Akt activation. Blood 132: 210-222, 2018.
36. Huang X, Zhou G, Wu W, Ma G, D'Amore PA, Mukai S and Lei H: Editing VEGFR2 blocks VEGF-induced activation of Akt and tube formation. Invest Ophthalmol Vis Sci 58: 1228-1236, 2017.
37. Hosseini-Koupaei M, Shareghi B, Saboury AA and Davar F: Molecular investigation on the interaction of spermine with proteinase K by multispectroscopic techniques and molecular simulation studies. Int J Biol Macromol 94: 406-414, 2017.
38. Liu D, Cao X, Kong Y, Mu T and Liu J: Inhibitory mechanism of sinensetin on α-glucosidase and non-enzymatic glycation: Insights from spectroscopy and molecular docking analyses. Int J Biol Macromol 166: 259-267, 2021.
39. Hu B, An HM, Wang SS, Chen JJ and Xu L: Preventive and therapeutic effects of Chinese herbal compounds against hepatocellular carcinoma. Molecules 21: 142, 2016.
40. Liao CY, Lee CC, Tsai CC, Hsueh CW, Wang CC, Chen IH, Tsai MK, Liu MY, Hsieh AT, Su KJ, *et al*: Novel investigations of flavonoids as chemopreventive agents for hepatocellular carcinoma. Biomed Res Int 2015: 840542, 2015.
41. Kim SM, Rampogu S, Vetrivel P, Kulkarni AM, Ha SE, Kim HH, Lee KW and Kim GS: Transcriptome analysis of sinensetin-treated liver cancer cells guided by biological network analysis. Oncol Lett 21: 355, 2021.
42. Hanahan D and Weinberg RA: Hallmarks of cancer: The next generation. Cell 144: 646-674, 2011.
43. Figueiredo CC, Pereira NB, Pereira LX, Oliveira LAM, Campos PP, Andrade SP and Moro L: Double immunofluorescence labeling for CD31 and CD105 as a marker for polyether polyurethane-induced angiogenesis in mice. Histol Histopathol 34: 257-264, 2019.
44. Salvucci O, Maric D, Economopoulou M, Sakakibara S, Merlin S, Follenzi A and Tosato G: EphrinB reverse signaling contributes to endothelial and mural cell assembly into vascular structures. Blood 114: 1707-1716, 2009.
45. Lam IK, Alex D, Wang YH, Liu P, Liu AL, Du GH and Lee SM: In vitro and in vivo structure and activity relationship analysis of polymethoxylated flavonoids: identifying sinensetin as a novel antiangiogenesis agent. Mol Nutr Food Res 56: 945-956, 2012.
46. Alon T, Hemo I, Itin A, Pe'er J, Stone J and Keshet E: Vascular endothelial growth factor acts as a survival factor for newly formed retinal vessels and has implications for retinopathy of prematurity. Nat Med 1: 1024-1028, 1995.
47. Hida K, Kawamoto T, Ohga N, Akiyama K, Hida Y and Shindoh M: Altered angiogenesis in the tumor microenvironment. Pathol Int 61: 630-637, 2011.
48. Poon RT, Fan ST and Wong J: Clinical implications of circulating angiogenic factors in cancer patients. J Clin Oncol 19: 1207-1225, 2001.
49. Rapisarda A and Melillo G: Role of the VEGF/VEGFR axis in cancer biology and therapy. Adv Cancer Res 114: 237-267, 2012.
50. Jászai J and Schmidt MHH: Trends and challenges in tumor anti-angiogenic therapies. Cells 8: 1102, 2019.
51. Boguslawski G, McGlynn PW, Harvey KA and Kovala AT: SU1498, an inhibitor of vascular endothelial growth factor receptor 2, causes accumulation of phosphorylated ERK kinases and inhibits their activity in vivo and in vitro. J Biol Chem 279: 5716-5724, 2004.
52. Zhang J, Cao J, Weng Q, Wu R, Yan Y, Jing H, Zhu H, He Q and Yang B: Suppression of hypoxia-inducible factor 1α (HIF-1α) by tirapazamine is dependent on eIF2α phosphorylation rather than the mTORC1/4E-BP1 pathway. PLoS One 5: e13910, 2010.